Proteins of the Innate Immune System Crystallize on Carbon Nanotubes but Are Not Activated

Wai Li Ling,*,†,‖,¶,‡ Adrienn Biro,†,‖,¶ Isabelle Bally,†,‖,¶ Pascale Tacnet,†,‖,¶ Aurélien Deniaud,†,‖,¶ Eric Doris,§ Philippe Frachet,†,‖,¶ Guy Schoehn,†,‖,¶,⊥ Eva Pebay-Peyroula,†,‖,¶ and Gérard J. Arlaud†,‖,¶

†CEA, Institut de Biologie Structurale Jean-Pierre Ebel, 38027 Grenoble, France, ‖CNRS, Institut de Biologie Structurale Jean-Pierre Ebel, 38027 Grenoble, France, ¶Université Joseph Fourier — Grenoble 1, Institut de Biologie Structurale Jean-Pierre Ebel, 38027 Grenoble, France, ‡CEA, LETI, Minatec, 38054 Grenoble Cedex 9, France, §CEA, iBiTecS, Service de Chimie Bioorganique et de Marquage, 91191 Gif-sur-Yvette, France, and ⊥Unit for Virus Host Cell Interaction, UMR 5233, Université Joseph Fourier, EMBL, CNRS, Grenoble, France

ABSTRACT The classical pathway of complement is an essential component of the human innate immune system involved in the defense against pathogens as well as in the clearance of altered self-components. Activation of this pathway is triggered by C1, a multimolecular complex comprising a recognition protein C1q associated with a catalytic subunit C1s-C1r-C1r-C1s. We report here the direct observation of organized binding of C1 components C1q and C1s-C1r-C1r-C1s on carbon nanotubes, an ubiquitous component in nanotechnology research. Electron microscopy imaging showed individual multiwalled carbon nanotubes with protein molecules organized along the length of the sidewalls, often over 1 μm long. Less well-organized protein attachment was also observed on double-walled carbon nanotubes. Protein-solubilized nanotubes continued to attract protein molecules after their surface was fully covered. Despite the C1q binding properties, none of the nanotubes activated the C1 complex. We discuss these results on the adsorption mechanisms of macromolecules on carbon nanotubes and the possibility of using carbon nanotubes for structural studies of macromolecules. Importantly, the observations suggest that carbon nanotubes may interfere with the human immune system when entering the bloodstream. Our results raise caution in the applications of carbon nanotubes in biomedicine but may also open possibilities of novel applications concerning the many biochemical processes involving the versatile C1 macromolecule.

KEYWORDS: carbon nanotubes · immunotoxicity · complement · C1q · C1s-C1r-C1r-C1s · 2D crystallization · nanotoxicity

Due to their particular structural, mechanical, and transport properties, carbon nanotubes (CNTs) have been exploited in innovative research ranging from renewable energy to medicine.[1,2] Single-walled CNTs (SWCNTs), composed of one layer of graphene cylinder, have a diameter of 1−2 nm and are relatively flexible, while multiwalled CNTs (MWCNTs), with multiple layers of concentric graphene cylinders, have diameters ranging from 2 to ∼100 nm and are more rigid. Often, CNTs are modified by covalent functionalization for specific applications. Nevertheless, as-grown CNTs with or without adsorbed molecules are also commonly employed. For example, as-grown MWCNTs protruding from an anodized Ti matrix can improve the performance of Ti orthopedic material.[3] Feasibility of using SWCNTs with adsorbed polyethylene oxide chains in electronic biomolecule detectors has also been demonstrated.[4] Considering their increasing range of applications and potential contact with the general population, understanding interactions of CNTs with human proteins is imperative.[5,6]

In addition to contact through the skin or inhalation when using or producing CNT devices, many applications intend to administer CNTs into the body internally.[2] These CNTs are expected to be in contact with serum proteins and, in particular, with proteins of the immune system.[7] In fact, some applications are designed to interact directly with the immune system. For example, CNTs are used in research for vaccination as well as gene and cancer therapy.[8−10] Understanding the interplay between CNTs and immune proteins is therefore critical for both improving CNT applications in biology and medicine and avoiding potentially noxious immune responses.

The C1 complex is an important component of the complement system, a group of serum proteins forming part of the innate immune system. Activation of the classical complement pathway is initiated by C1 and triggers a cascade of proteolytic reactions resulting in the clearance of the target. C1 comprises two interacting subunits: a recognition protein C1q and a proenzyme tetrameric complex C1s-C1r-C1r-C1s assembled from two proteases C1r and C1s.[11,12] The cascade activated upon binding of C1q to the targets leads to their opsonization allowing their phagocytosis and to the recruitment of other components of the immune system. Whereas macrophages mostly recognize surface molecules common to many pathogens, C1q senses a wide range of foreign

*Address correspondence to wai-li.ling@ibs.fr.

Received for review March 26, 2010 and accepted December 20, 2010

Published online January 07, 2011
10.1021/nn102400w

objects as well as altered or unwanted self-cells or materials through its multivalent globular head domains (see below). Indeed, besides pathogen defense, C1q is involved in many crucial processes and disorders.[13] For example, C1q recognizes danger signals on apoptotic cells as well as damaged low-density lipoproteins (LDL) in early atherosclerosis.[14−16] C1q also recognizes amyloid fibrils and abnormal prion proteins and is thought to be involved in neurodegenerative processes, including Alzheimer's disease.[17−19] On the other hand, C1 deficiency leads to autoimmune diseases, most notably systemic lupus erythematosus.[20] All these considerations prompted us to investigate the interaction of C1q and its partner C1s-C1r-C1r-C1s with CNTs.

Structurally, C1q is hexameric and contains six copies of each of three distinct polypeptide chains. The amino terminal ends of the 18 chains associate to form a collagen stalk. The stalk diverges to form six individual arms where the collagen sequence of the chains is interrupted, resulting in semiflexible joints.[21,22] Each of the six arms is made up of one copy of each of the three chains, and the carboxyl terminals of the three chains form a globular domain. The globular heads are approximately 6 nm wide and have multivalent charged groups for target recognition. The hexameric structure of C1q allows target binding by multiple heads. The whole C1q molecule is ~460 kDa and measures around 40 nm across.

When activated upon target binding of C1q, C1s-C1r-C1r-C1s turns into an enzyme that starts the complement cascade. C1r and C1s are homologous proteins and, in the presence of Ca^{2+}, form a tetramer, which is a linear arrangement C1s-C1r-C1r-C1s.[23] It is proposed that in the C1 complex, the extended tetramer has multiple interaction sites with C1q and folds into a compact double loop inside the cone enclosed by the six collagen arms of C1q.[24] In the free tetramer, a C1s molecule, which resembles a dumbbell, is found on each of the two sides of the X-shaped C1r-C1r dimer.[23] The tetramer is ~330 kDa and is roughly 50 × 25 × 5 nm in size in its extended conformation.

We present transmission electron microscopy (EM) studies on the binding of C1 components on commercially available SWCNTs, double-walled CNTs (DWCNTs) and MWCNTs. These analyses reveal that both C1q and C1s-C1r-C1r-C1s bind to the surface of MWCNTs in an organized fashion. On the other hand, C1q binds neither to DW nor to SWCNTs, and C1s-C1r-C1r-C1s binds to DW but not to SWCNTs. Besides the ordered packing of the first monolayer on the CNTs, we found that proteins continued to stack on the fully covered CNTs, thereby depleting the proteins in the solution. Independent of the results of the binding experiments, we found that all CNTs failed to activate the C1 complex *in vitro*. These results on protein−CNT interactions may lead to new possibilities and questions in the biomedical applications of CNTs.

RESULTS AND DISCUSSION

We investigated the interaction of the two subunits of the complement activation protein C1-C1q and C1s-C1r-C1r-C1s, with three different types of nanotubes MW, DW, and SWCNTs. Due to its tendency to dissociate, C1 has not been successfully observed by EM without prior chemical cross-linking.[25] We therefore investigated the interactions of the two C1 subunits with CNTs individually.

We first looked at the interaction of CNTs with C1q. Electron micrographs and drawings of C1q are shown in Figure 1A. Whereas the globular heads and the collagen stalk could be observed quite easily with EM, the thin arms connecting the heads to the stalk were not always visible as they were easily damaged by radiation and not always in good contact with the carbon support film. Images of C1q molecules thus appeared usually as clusters of six globes, with the stalk appearing sometimes as an extra globe depending on its orientation on the support film.

MWCNTs were readily suspended to form a homogeneous black solution upon sonication with C1q but not with the buffer alone. (Dissolution of CNTs also occurred with agitation of the mixture only but was sped up by sonication.) The MWCNT plus protein solution was centrifuged, and the pellet was resuspended in the triethanolamine buffer to remove excess proteins. This washing procedure was usually repeated. The CNTs were immediately stained and imaged with EM before protein desorption. Different stains, including sodium silicotungstate (pH 7.4), uranyl acetate (pH 4.5), and ammonium molybdate (pH 7.5), all gave similar results. Buffers with and without Ca^{2+} ions also gave similar results.

Individual MWCNTs could be found routinely in the resuspended MWCNT solution, with organized C1q patterns dominated by bead-like structures. (The contrast in appearance between a protein-covered sidewall and the smooth bare sidewall is shown in an image of a MWCNT partly covered with proteins in Figure S1, Supporting Information.) Typical images of the resuspended MWCNTs are found in Figure 1. Comparison of the `beads' to the globular domains of free C1q molecules close-by strongly suggests that they are the globular domains bound to the MWCNT surface (Figure 1B and right inset of Figure 1C). Upon close inspection, the fine arms emanating from the globular heads in the adsorbed molecules can also be discerned (see left magnified image in Figure 1C).

From our EM observation, organized molecules often covered the full length of the MWCNTs. These overlayers were generally organized well enough to yield diffraction patterns in their power spectra. In our CNTs samples, which have a distribution of diameters, we have observed C1q crystallization on MWCNTs of various diameters. For example, the decorated nanotube in Figure 1B has a diameter ~45 nm and that in

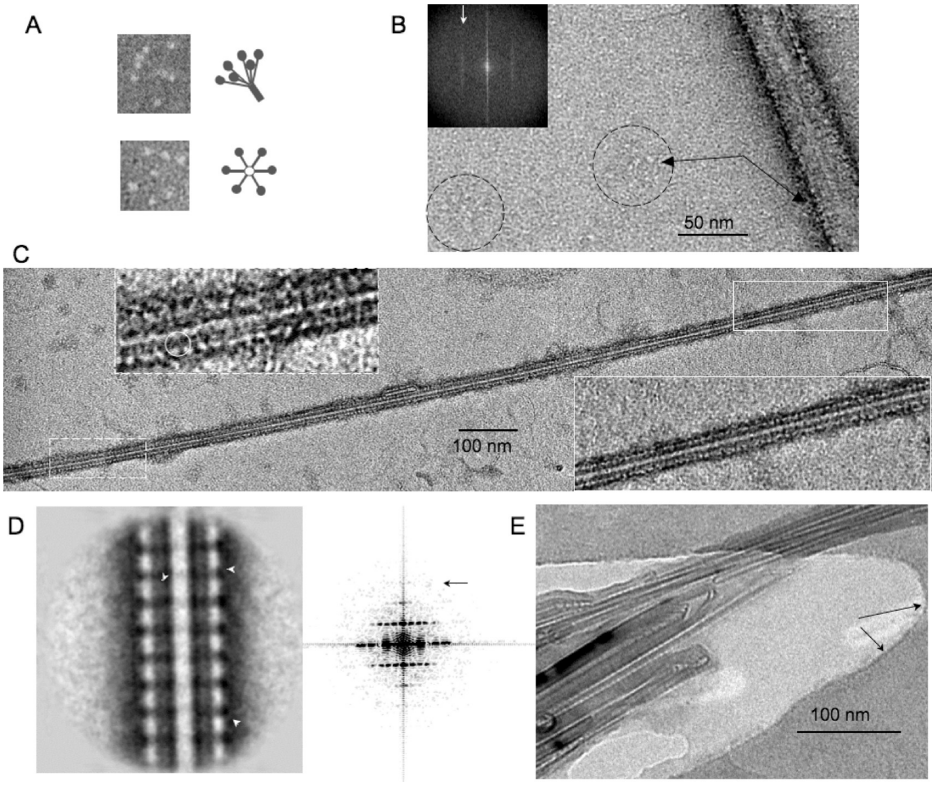

Figure 1. Interaction of C1q molecules with MWCNTs. (A) Electron micrographs and schematic representations of side (top) and top (bottom) views of the C1q molecule, which consists of a collagen stalk spreading out to six equivalent arms ending in globular head domains. (B) Portion of a C1q-covered MWCNT along with free C1q molecules. A C1q molecule lying on its side with its six heads fanned out flat on the support film (circled left) and another one appearing as a cluster of its globular heads (circled center) can be found on the left of the nanotube. Inset shows power spectrum of the covered nanotube with arrow pointing to a diffraction line at ~1/6 nm. (C) Portion of a MWCNT with C1q molecules organized along the ~1.5 μm field of view. Insets show magnified views of the covered nanotube with discerned collagen arms circled in the left inset. (D) Averaged view of the C1q organization on the MWCNT in (C) and its power spectrum. White arrowheads point to examples of discerned collagen arms in the image, and the black arrow points to the third diffraction line resolved at 1/19 Å. (E) Cryo-electron micrograph of a MWCNT bundle embedded in vitrified buffer suspended in a hole of a lacey carbon film. The arrows point to the edge of the carbon film. Organized C1q molecules cover the nanotubes as in negatively stained samples. The long straight lines running along the bundle correspond to the nanotube walls.

Figure 1C ~25 nm. Assuming they have only one monolayer of C1q, the nanotubes themselves are ~35 and ~15 nm in diameter, respectively. Figure 1D shows the organization of the C1q molecules on the MWCNT surface in Figure 1C averaged using ~100 images along the nanotube. The computed power spectrum shows three layer lines 1/5.6 nm apart, with a strong diffraction signal at the meridian corresponding to rings of width close to the size of the globular domain of the C1q molecules. Fine arms connecting the globular domains to the collagen stems can also be discerned in the averaged image. Nonetheless, because the collagen stems conceivably had collapsed in random directions in these negatively stained samples, their positions were ill-defined, giving rise to an important background in the power spectra.

Vitrified samples also showed the same organization on the CNT surface (Figure 1E). No stain was applied in these samples. Unlike in the negatively stained samples where the images are dominated by contrast from stained surface proteins, the cryo-image presents a real projection through the volume of the CNTs. The protein molecules here show only weak contrast, and the graphene layers of the underlying MWCNTs can be seen clearly in the image. As shown in the example in Figure 1E, the CNTs were highly bundled in the vitrified samples.

We repeated the experiment with DW and SWCNTs, but neither sample was suspended in the C1q solution. Even though the globular heads may bind to the graphene side wall as on the MWCNT surface, robust attachment through multiple heads on the SW or DWCNTs would not be expected considering the sizes of the nanotubes ($Ø_{DW}$ ~5 and $Ø_{SW}$ ~1 nm) relative to the dimensions and geometry of the C1q molecules.

The ability of SW, DW, and MWCNTs to trigger activation of the C1 complex was investigated using an *in vitro* assay.[26] As sonication was found to speed up dispersion of MWCNTs in the presence of C1q, C1 activation was initially tested with and without prior sonication of the reaction mixtures. Incubation of C1 with each CNT species at ~3 mg/mL did not significantly

activate C1 under either condition, although a slight increase over background activation was observed for the sonicated MWCNT sample (Figure 2A). However, further analysis in the presence of increasing MWCNT concentrations did not show evidence that MWCNTs were able to significantly activate C1 at concentrations up to 20 mg/mL (Figure 2B).

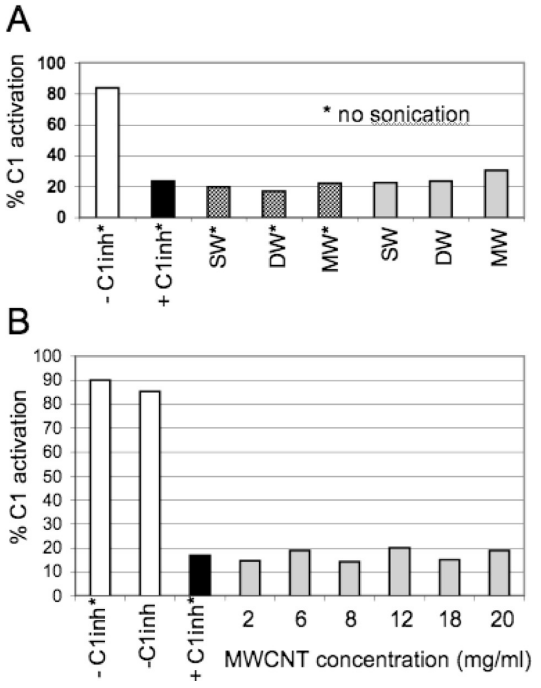

Figure 2. CNTs do not trigger C1 activation. The ability of the three CNT species to activate C1 was tested using an *in vitro* assay. (A) C1 activation by SW, DW, and MWCNTs (each 3.2 mg/mL). A positive control (in the absence of C1 inhibitor) and a negative control (in the presence of excess C1 inhibitor) are shown. Reaction mixtures were sonicated except when indicated by asterisks. (B) C1 activation by increasing concentrations of MWCNTs.

Efficient C1 activation by a target is known to require multivalent binding through several C1q globular heads and is thought to involve deformation of the C1q collagen region, imparting a mechanical stress in C1r and thereby triggering its activation.[11] Thus, that MWCNTs fail to activate C1 may arise from the fact that the globular heads of C1q bind in a symmetric manner on the CNT surface, which impedes C1 activation. The fact that, in addition to C1q, the C1s-C1r-C1r-C1s tetramer also binds to MWCNTs (see below) may also weaken the C1 complex, resulting in C1 dissociation and thereby preventing activation. On the other hand, it cannot be excluded that the assembled C1 complex does not bind to the MWCNT surface, contrary to free C1q. Further investigations will be required to address this issue.

It is noteworthy that DW and SWCNTs have been shown to be soluble in serum and to activate the classical complement pathway at concentrations lower than that used in our C1 activation assays.[27] As these experiments were based on hemolytic assays using whole serum as a source of complement, it cannot be excluded that other serum proteins form a stable overlayer on the CNTs, thereby allowing their solubilization and triggering indirect C1 binding and activation. (Figure S2, Supporting Information, shows an example of C1q binding to its ligand calreticulin organized on the MWCNT surface.) In our hands, despite the binding properties observed for the different types of CNTs, none of them significantly activated C1 directly.

We next investigated the binding of the proenzyme C1s-C1r-C1r-C1s tetramer to CNTs. A drawing of the free tetramer is found in Figure 3A. MWCNTs were also readily suspended in the C1s-C1r-C1r-C1s solution. Interestingly, an organized overlayer was also found covering the full length of individual MWCNTs. Examples are shown in Figure 3 for CNTs of diameters ~28

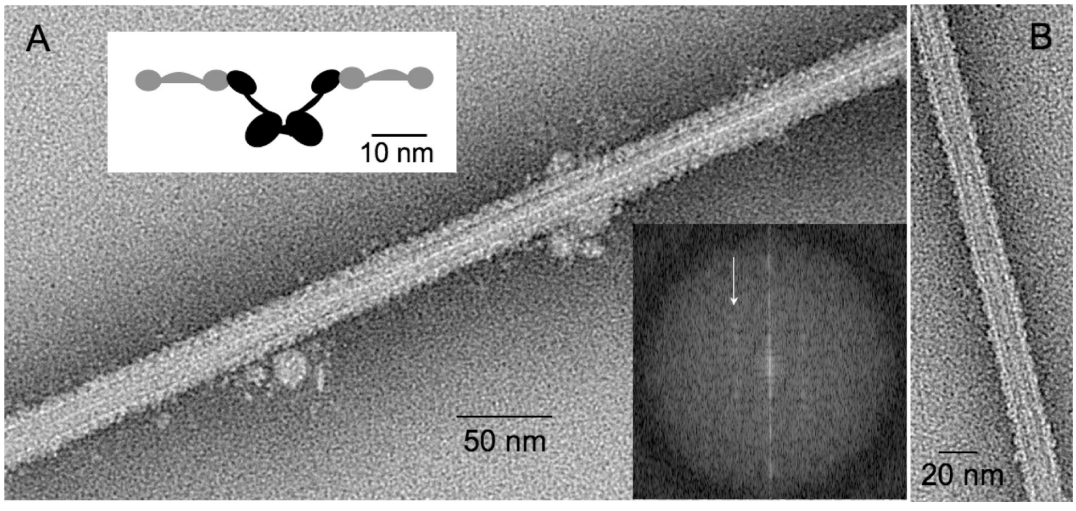

Figure 3. The C1s-C1r-C1r-C1s tetramer bound to MWCNTs. (A) Top-left inset shows a schematic representation of the tetramer, with a dumbbell-shaped C1s (gray) on each of the two sides of the C1r-C1r dimer (black), which forms an X-shape (adapted from Weiss *et al.*, 1986). Power spectrum (rotated with respect to the image) shows a layer line (white arrow) at ~1/8 nm. (B) A nanotube of smaller diameter also shows organized protein attachment.

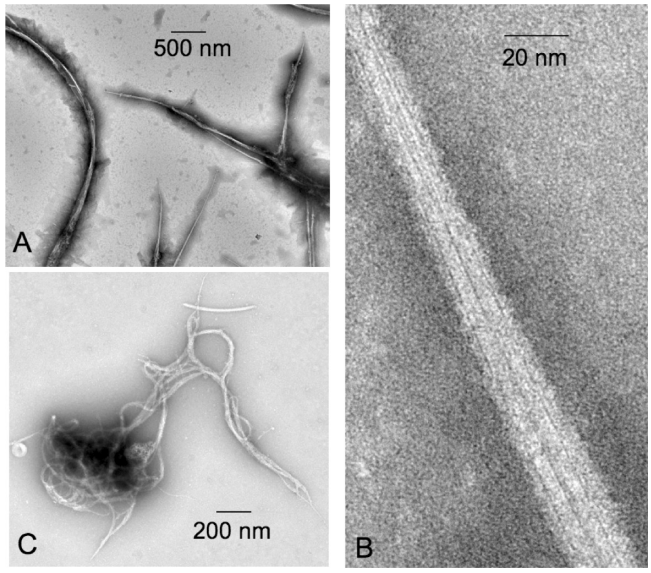

Figure 4. The C1s-C1r-C1r-C1s tetramer on DW and SWCNTs. (A) DWCNTs suspended in the C1s-C1r-C1r-C1s solution remain bundled and entangled. (B) Surface of DWCNT bundle shows striations suggesting that the proteins attach in an organized fashion. (C) A large cluster of highly entangled SWCNTs found in the supernatant of the C1s-C1r-C1r-C1s solution.

and ~13 nm (Figure 3A and B, respectively). Power spectra of both nanotubes show a layer line at around 1/8 nm, as illustrated for the nanotube in Figure 3A. Considering the shape of the tetramer, the layer line would suggest that the molecules wrap around the CNTs with a pitch of 8 nm. The C1r-C1r dimer might have collapsed during the sample preparation in this structure, which would contribute to the noisy power spectra.

DWCNTs were also suspended in solutions of the C1s-C1r-C1r-C1s tetramer, but the nanotubes remained in bundles, as shown in Figure 4A. Striations could be seen on some of the surfaces of the bundles, suggesting adsorbate organization (Figure 4B). A similar organization on DWCNTs bundles has also been observed for pulmonary surfactant proteins.[28] SWCNTs did not form any good suspension in C1s-C1r-C1r-C1s solutions, and the light gray supernatant in the solution only yielded highly entangled clumps of SWCNTs.

When suspended CNTs were left in protein solution, we found that protein molecules continued to attach to the fully covered nanotube surface. Figure 5 shows a typical MWCNT left in the C1q solution for one week. On the contrary, when protein-covered CNTs were left in buffer alone, the overlayer disorganized and desorbed with time.

Balavoine *et al.* have proposed to use protein crystallization on CNTs for structural studies of proteins by helical reconstruction with EM analysis.[29] Such structural analysis potentially has a number of advantages over traditional methods. For instance, the signal-to-noise ratio will significantly improve with the periodicity. Moreover, collection of EM images at different tilt angles, which causes considerable radiation damage, will be unnecessary because of the multiple views of the molecule present on a helix. Whereas streptavidin

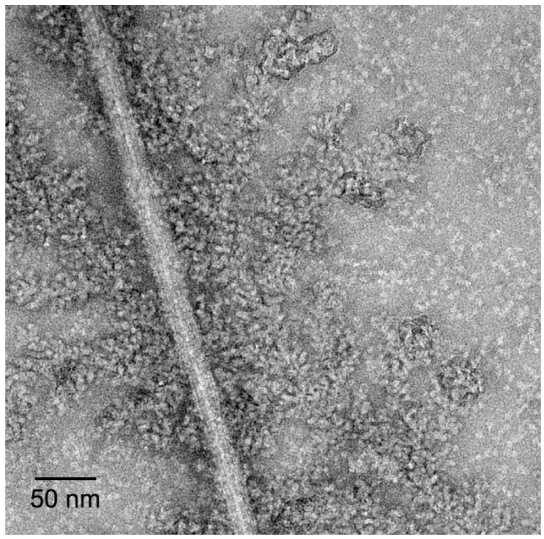

Figure 5. CNTs continue to attract protein molecules after sidewalls are fully covered. A MWCNT incubated with C1q molecules for one week. Organized protein molecules on the surface of the nanotube act as `seeds' as dendritic growth emanates from the nanotube surface.

and HupR used by Balavoine *et al.* have been crystallized in two (2D) and three-dimensions (3D) and have known structures, C1q and C1s-C1r-C1r-C1s have not been successfully crystallized, and their structures have not been solved. The crystallization of these human immune proteins on CNTs is thus very encouraging for pursuing this original technique for structural studies of macromolecules.

Whereas the order of the C1 components on CNT surface is limited by their flexible domains in the negatively stained samples, well-organized helix could be observed with the compact globular domain of C1q. Figure 6 shows a single-stranded helix of radius ~8 nm

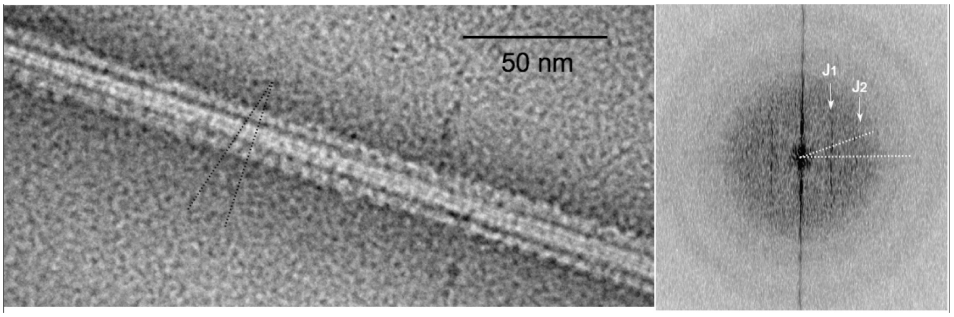

Figure 6. Helical organization of C1q globular head domains on MWCNTs and the computed power spectrum (rotated with respect to the image). Dotted lines show the inclination of the helix, and the two white arrows show the location of the first- and second-order Bessel functions.

and pitch ~7 nm formed by the C1q globular domain on a MWCNT. The first maxima of the first and second order Bessel functions of the principal branch can be identified. Nonetheless, the noisy power spectrum suggests the apparent presence of various helical domains. Further experiments will be necessary to obtain better quality crystals amenable to structural analyses,[30−32] but this is beyond the scope of this communication.

In summary, we have shown that the two components of the complement activation complex C1 form ordered overlayers on MWCNTs. Less-ordered binding was also found on bundles of DWCNTs for proenzyme C1s-C1r-C1r-C1s, while a well-defined helix was found on MWCNTs with the globular domain of C1q. Protein continued to accumulate around the nanotubes even after their surface was fully covered. Irrespective of the different binding properties for the three types of CNTs studied, we found no significant C1 activation using the three CNT samples.

Considering that MWCNTs readily bind and attract C1q and C1s-C1r-C1r-C1s, they would be likely to interfere with the activation of the complement system. Whether this will lead to a depletion of the activation proteins *in vivo* will be an important question to answer in future studies. It would also be important to know whether the whole C1 complex and other molecules of the complement cascade also bind to CNTs. These questions will need to be addressed for the safe adoption of CNT devices. On the other hand, the self-assembly of C1q on the CNT surface may open possibilities of novel CNT applications concerning the many biochemical processes that involve the C1 complex.

Adsorption of organic molecules on CNTs is still poorly understood.[33] Charge transfer was shown in the interaction between CNTs and streptavidin, which organizes helically on MWCNT.[34] Hydrophobic interaction is also likely in effect for streptavidin binding.[29] These factors, in particular charge transfer, most probably played a role in the binding of the protein molecules we studied here, especially in the case of C1q, which has multiple-charged groups on its globular heads.[13] Other factors, such as chirality and the presence of functional groups or ions, have been suggested to also play a role in the adsorption and organization of organic molecules on CNTs in general.[33] Even though we used nonfunctionalized CNTs in our studies, functional groups may be present from the synthesis or purification process. These functional groups may act as nucleation sites for protein binding but are unlikely to lead to ordering. Chirality of the outer graphene layer may also govern the affinity of protein molecules but probably not protein organization, considering the large size of protein domains.

From previously published results and from our own observations, we propose that interaction among the protein molecules may be a factor to consider in the formation of a stable overlayer on the CNT surface. Crystallization of macromolecules on CNTs has been associated with noncovalently solubilized CNTs.[28,29] Besides protein molecules, surfactants have also been found to solubilize CNTs forming ordered rings of half-micelles around the nanotubes.[35] In this work, we showed that C1 components can also organize on the surface of solublized CNTs. Figure S3, Supporting Information, shows more examples of organized protein overlayers found on CNTs that form a stable suspension in the protein solution. Thus, while the factors discussed before may contribute to the adsorption of macromolecules on the CNT surface, attraction among the adsorbed molecules may be necessary to maintain a stable overlayer of the macromolecules, which allows the solubilization of the CNTs. Nonetheless, crystals were found in only some but not all of the solubilized CNTs. Further experimental and theoretical studies will be needed to fully understand these issues.

METHODS

SWCNTs and DWCNTs (produced by catalytic carbon vapor deposition) were purchased from Nanocyl S.A. (Namur, Belgium), and MWCNTs (produced by arc-discharge) were purchased from n-Tec Scandinavian Advanced Technology (Oslo, Norway). The modal diameters of the SW, DW and

MWCNTs are, respectively, ~1, ~5, and ~25 nm. Residual carbonaceous impurities were removed by washing in methanol, and the cleaned CNTs were dried before protein applications.

Details of the reagents and proteins were described previously.[17,24,36,37] The C1q recognition subunit of C1 and proenzymes C1r and C1s were purified from human plasma, and the tetrameric complex C1s-C1r-C1r-C1s was then reconstituted in the presence of Ca^{2+}. The proteins were dialyzed in 50 mM triethanolamine−HCl, 145 mM NaCl, 0.5 mM $CaCl_2$, and pH 7.4. Concentrations of the purified proteins were determined as previously described[26] and were around 0.3−0.5 mg/mL. The homogeneity of the purified proteins was assessed by sodium dodecyl sulfate-polyacrylamide gel electrophoresis (SDS-PAGE) analysis under reducing and nonreducing conditions and by EM. The ability of CNTs to trigger C1 activation was measured using an *in vitro* assay, as described previously.[28] Briefly, C1 was reconstituted from purified C1q and proenzyme C1s-C1r-C1r-C1s. The complex (0.25 μM) was incubated in 50 mM triethanolamine−HCl, 145 mM NaCl, 1 mM $CaCl_2$, and pH 7.4 for 90 min at 37 °C in the presence of 1 μM C1 inhibitor and various CNT concentrations. The extent of activation was measured by SDS-PAGE followed by Western blot analysis using an anti-C1s antibody.

The globular domain of human C1q was generated essentially as described by Tacnet *et al.*[17] Briefly, C1q was treated with collagenase (C1q:collagenase ratio = 15:1, w/w) for 16 h at 37 °C, and purification was achieved by high-pressure gel permeation on a TSK-G2000 SW column (LKB).

The solubility of CNTs in the protein solution was used as a test of binding. Nanotubes were mixed into the protein solution and gently sonicated. Solubilized CNTs were centrifuged, resuspended in the buffer, and imaged immediately using the negative-staining technique. Small volumes (2−4 μL) of the samples were adsorbed onto the clean face of a carbon film deposited on cleaved mica. The carbon film was then floated in the stain solution and laid on an EM grid. The negatively stained specimens were examined using a Philips CM12 LaB_6 electron microscope operating at 120 kV. Images were recorded on Kodak electron image films SO-163 or using a Gatan Orius CCD camera with a pixel size of 9 μm (0.2 nm at the sample scale). Images on films were digitalized on a Zeiss scanner with a pixel size of 7 μm on the micrograph corresponding to 1.6 Å for images taken at 45 kX magnification. Grids for cryo-EM were prepared by applying a small volume (2−4 μL) of sample onto a grid with a lacey carbon film. The grid was then plunge-frozen in liquid ethane after removal of excess liquid. Frozen grids were observed by cryo-EM under low-dose conditions (<20 electrons/$Å^2$) using a Philips CM200 LaB6 electron microscope at 200 kV, and images were recorded on films. Fourier transforms and power spectra were obtained using ImageJ. Images of C1q on MWCNT were boxed and averaged using SPIDER, as described in Bartual *et al.*[38,39] The best 50%, as judged by cross-correlation of about 100 images, were averaged, and the procedure was repeated for 10 cycles.

Acknowledgment. The authors thank J.-P. Bourgoin and A. Chabli for support and E. A. Hewat and J. Navaza for discussion. The work has been partly funded by the Transverse Nanoscience Program of CEA.

Supporting Information Available: Three additional figures showing protein-bound vs bare CNT (Figure S1), C1q binding on its ligands organized on MWCNTs (Figure S2), and other protein organizations on MWCNTs (Figure S3). This material is available free of charge *via* the Internet at http://pubs.acs.org.

REFERENCES AND NOTES

1. Sgobba, V.; Guldi, D. M. Carbon Nanotubes-Electronic/Electrochemical Properties and Application for Nanoelectronics and Photonics. *Chem. Soc. Rev.* **2009,** *38*, 165–184.
2. Tran, P. A.; Zhang, L.; Webster, T. J. Carbon Nanofibers and Carbon Nanotubes in Regenerative Medicine. *Adv. Drug Delivery Rev.* **2009,** *61*, 1097–1114.
3. Sirivisoot, S.; Yao, C.; Xiao, X.; Sheldon, B. W.; Webster, T. J. Greater Osteoblast Functions on Multiwalled Carbon Nanotubes Grown from Anodized Nanotubular Titanium for Orthopedic Applications. *Nanotechnology* **2007,** *18*, 365102–365102.
4. Chen, R. J.; Bangsaruntip, S.; Drouvalakis, K. A.; Wong Shi Kam, N.; Shim, M.; Li, Y.; Kim, W.; Utz, P. J.; Dai, H. Noncovalent Functionalization of Carbon Nanotubes for Highly Specific Electronic Biosensors. *Proc. Natl. Acad. Sci. U.S.A.* **2003,** *100*, 4984–4989.
5. Nel, A.; Xia, T.; Madler, L.; Li, N. Toxic Potential of Materials at the Nanolevel. *Science* **2006,** *311*, 622–627.
6. Lewinski, N.; Colvin, V.; Drezek, R. Cytotoxicity of Nanoparticles. *Small* **2008,** *4*, 26–49.
7. Dobrovolskaia, M. A.; McNeil, S. E. Immunological Properties of Engineered Nanomaterials. *Nat. Nanotech.* **2007,** *2*, 469–478.
8. Pantarotto, D.; Partidos, C. D.; Hoebeke, J.; Brown, F.; Kramer, E.; Briand, J.-P.; Muller, S.; Prato, M.; Bianco, A. Immunization with Peptide-Functionalized Carbon Nanotubes Enhances Virus-Specific Neutralizing Antibody Responses. *Chem. Biol.* **2003,** *10*, 961–966.
9. Kam, N. W. S.; Dai, H. Carbon Nanotubes as Intracellular Protein Transporters: Generality and Biological Functionality. *J. Am. Chem. Soc.* **2005,** *127*, 6021–6026.
10. Liu, Z.; Cai, W.; He, L.; Nakayama, N.; Chen, K.; Sun, X.; Chen, X.; Dai, H. *In Vivo* Biodistribution and Highly Efficient Tumour Targeting of Carbon Nanotubes in Mice. *Nat. Nanotech.* **2007,** *2*, 47–52.
11. Gaboriaud, C.; Thielens, N. M.; Gregory, L. A.; Rossi, V.; Fontecilla-Camps, J. C.; Arlaud, G. J. Structure and Activation of the C1 Complex of Complement: Unraveling the Puzzle. *Trends Immunol.* **2004,** *25*, 368–373.
12. Ziccardi, R. J. The First Componennt of Human Complement (C1): Activation and Control. *Springer Semin. Immunopathol.* **1983,** *6*, 213–230.
13. Kishore, U.; Gaboriaud, C.; Waters, P.; Shrive, A. K.; Greenhough, T. J.; Reid, K. B. M.; Sim, R. B.; Arlaud, G. J. C1q and Tumor Necrosis Factor Superfamily: Modularity and Versatility. *Trends Immunol.* **2004,** *25*, 551–561.
14. Taylor, P. R.; Carugati, A.; Fadok, V. A.; Cook, H. T.; Andrews, M.; Carroll, M. C.; Savill, J. S.; Henson, P. M.; Botto, M.; Walport, M. J. A Hierarchical Role for Classical Pathway Complement Proteins in the Clearance of Apoptotic Cells *in Vivo*. *J. Exp. Med.* **2000,** *192*, 359–366.
15. Paidassi, H.; Tacnet-Delorme, P.; Garlatti, V.; Darnault, C.; Ghebrehiwet, B.; Gaboriaud, C.; Arlaud, G. J.; Frachet, P. C1q Binds Phosphatidylserine and Likely Acts as a Multiligand-Bridging Molecule in Apoptotic Cell Recognition. *J. Immunol.* **2008,** *180*, 2329–2338.
16. Biro, A.; Ling, W. L.; Arlaud, G. r. J. Complement Protein C1q Recognizes Enzymatically Modified Low-Density Lipoprotein through Unesterified Fatty Acids Generated by Cholesterol Esterase. *Biochemistry* **2010,** *49*, 2167–2176.
17. Tacnet-Delorme, P.; Chevallier, S.; Arlaud, G. J. β-Amyloid Fibrils Activate the C1 Complex of Complement Under Physiological Conditions: Evidence for a Binding Site for Aβ on the C1q Globular Regions. *J. Immunol.* **2001,** *167*, 6374–6381.
18. Beek, J.; Elward, K.; Gasque, P. Activation of Complement in the Central Nervous System. *Ann. N.Y. Acad. Sci.* **2003,** *992*, 56–71.
19. Erlich, P.; Dumestre-Pérard, C.; Ling, W. L.; Lemaire-Vieille, C.; Schoehn, G.; Arlaud, G. J.; Thielens, N. M.; Gagnon, J.; Cesbron, J.-Y. Complement Protein C1q Forms a Complex with Cytotoxic Prion Protein Oligomers. *J. Biol. Chem.* **2010,** *285*, 19267–19276.
20. Agostoni, A.; Cicardi, M. Hereditary and Acquired C1-Inhibitor Deficiency - Biological and Clinical Characteristics in 235 Patients. *Medicine* **1992,** *71*, 206–215.
21. Shelton, E.; Yonemasu, K.; Stroud, R. M. Ultrastructure of the Human Complement Component, Clq. *Proc. Natl. Acad. Sci. U.S.A.* **1972,** *69*, 65–68.
22. Reid, K. B.; Porter, R. R. Subunit Composition and Structure of Subcomponent C1q of the First Component of Human Complement. *Biochem. J.* **1976,** *155*, 19–23.

23. Weiss, V.; Fauser, C.; Engel, J. Functional Model of Subcomponent C1 of Human Complement. *J. Mol. Biol.* **1986,** *189*, 573–581.
24. Bally, I.; Rossi, V.; Lunardi, T.; Thielens, N. M.; Gaboriaud, C.; Arlaud, G. J. Identification of the C1q-binding Sites of Human C1r and C1s. *J. Biol. Chem.* **2009,** *284*, 19340–19348.
25. Strang, C. J.; Siegel, R. C.; Phillips, M. L.; Poon, P. H.; Schumaker, V. N. Ultrastructure of the First Component of Human Complement: Electron Microscopy of the Cross-linked Complex. *Proc. Natl. Acad. Sci. U.S.A.* **1982,** *79*, 586–590.
26. Biró, A.; Thielens, N. M.; Cervenák, L.; Prohászka, Z.; Füst, G.; Arlaud, G. J. Modified Low Density Lipoproteins Differentially Bind and Activate the C1 Complex of Complement. *Mol. Immunol.* **2007,** *44*, 1169–1177.
27. Salvador-Morales, C.; Flahaut, E.; Sim, E.; Sloan, J.; Green, M. L. H.; Sim, R. B. Complement Activation and Protein Adsorption by Carbon Nanotubes. *Mol. Immunol.* **2006,** *43*, 193–201.
28. Salvador-Morales, C.; Townsend, P.; Flahaut, E.; Vénien-Bryan, C.; Vlandas, A.; Green, M. L. H.; Sim, R. B. Binding of Pulmonary Surfactant Proteins to Carbon Nanotubes; Potential for Damage to Lung Immune Defense Mechanisms. *Carbon* **2007,** *45*, 607–617.
29. Balavoine, F.; Schultz, P.; Richard, C.; Mallouh, V.; Ebbesen, T. W.; Mioskowski, C. Helical Crystallization of Proteins on Carbon Nanotubes: A First Step towards the Development of New Biosensors. *Angew. Chem., Int. Ed.* **1999,** *38*, 1912–1915.
30. Yonekura, K.; Toyoshima, C.; Maki-Yonekura, S.; Namba, K. GUI Programs for Processing Individual Images in Early Stages of Helical Image Reconstruction--for High-resolution Structure Analysis. *J. Struct. Bio.* **2003,** *144*, 184–194.
31. Carragher, B.; Whittaker, M.; Milligan, R. A. Helical Processing Using PHOELIX. *J. Struct. Bio.* **1996,** *116*, 107–112.
32. Egelman, E. H. The Iterative Helical Real Space Reconstruction Method: Surmounting the Problems Posed by Real Polymers. *J. Struct. Bio.* **2007,** *157*, 83–94.
33. Pan, B.; Xing, B. Adsorption Mechanisms of Organic Chemicals on Carbon Nanotubes. *Environ. Sci. Technol.* **2008,** *42*, 9005–9013.
34. Bradley, K.; Briman, M.; Star, A.; Gruner, G. Charge Transfer from Adsorbed Proteins. *Nano Lett.* **2004,** *4*, 253–256.
35. Richard, C.; Balavoine, F.; Schultz, P.; Ebbesen, T. W.; Mioskowski, C. Supramolecular Self-Assembly of Lipid Derivatives on Carbon Nanotubes. *Science* **2003,** *300*, 775–778.
36. Arlaud, G. J.; Sim, R. B.; Duplaa, A.-M.; Colomb, M. G. Differential elution of Clq, Clr and Cls from human CT bound to immune aggregates. use in the rapid purification of Cl sub-components. *Mol. Immunol.* **1979,** *16*, 445–450.
37. Arlaud, G. J.; Villiers, C. L.; Chesne, S.; Colomb, M. G. Purified Proenzyme C1r. Some Characteristics of Its Activation and Subsequent Proteolytic Cleavage. *Biochim. Biophys. Acta* **1980,** *616*, 116–129.
38. Frank, J.; Radermacher, M.; Penczek, P.; Zhu, J.; Li, Y.; Ladjadj, M.; Leith, A. SPIDER and WEB: Processing and Visualization of Images in 3D Electron Microscopy and Related Fields. *J. Struct. Bio.* **1996,** *116*, 190–199.
39. Galan Bartual, S.; Garcia-Doval, C.; Alonso, J.; Schoehn, G.; van Raaij, M. J. Two-chaperone Assisted Soluble Expression and Purification of the Bacteriophage T4 Long Tail Fibre Protein gp37. *Protein Expr. Purif.* **2010,** *70*, 116–121.